

High-frequency dielectric constant of layered Fe, Co, and Ni dihalides

I. Pollini

Gruppo Nazionale di Struttura della Materia del Consiglio Nazionale delle Ricerche, Dipartimento di Fisica dell'Università degli Studi di Milano, Via Celoria 16, I-20133 Milano, Italy
and Laboratoire d'Utilisation du Rayonnement Electromagnétique, Université de Paris—Sud, F-91405 Orsay, France

G. Benedek

Gruppo Nazionale di Struttura della Materia del Consiglio Nazionale delle Ricerche, Dipartimento di Fisica dell'Università degli Studi di Milano, Via Celoria 16, I-20133 Milano, Italy

J. Thomas

Laboratoire de Spectroscopie, Université de Rennes I, F-35042 Rennes, France,
and Laboratoire d'Utilisation du Rayonnement Electromagnétique, Université de Paris—Sud, F-91405 Orsay, France

(Received 18 July 1983)

The high-frequency dielectric constants of layered Fe, Co, and Ni dihalides are obtained in the region 2–31 eV by Kramers-Kronig analysis of near-normal-incidence reflectance spectra measured with synchrotron radiation. The primary data may be described unambiguously in terms of single-particle excitations, as charge-transfer and interband transitions, and plasma resonance effects. Consideration of the sum rules involving the imaginary part of the dielectric function, $N_{\text{eff}}(E)$, and $\epsilon_{\text{eff}}(E)$ (the effective electron number and dielectric constant) was taken in order to permit comparison between experimental and theoretical results. A general good agreement was found with the extended-shell-model predictions based on transferable sets of polarizabilities for both anions and cations. The role of static dipoles is finally discussed in connection with the sizable deviations from the isotropic Clausius-Mossotti relation.

I. INTRODUCTION

The fundamental reflectance spectra of transition-metal halide (TMH) crystals with layered structure, recently measured in the range 2–31 eV by means of synchrotron radiation,^{1–3} allow an accurate determination of the high-frequency constants through the saturation value of the effective dielectric constant ϵ_{eff} . This is obtained above the reststrahlen frequency as a consequence of Kramers-Kronig (KK) relations and for finite intervals of integration.^{4–6} The experimental information, beside its intrinsic value, offers a useful test for the extended-shell model (ESM) recently employed for the lattice dynamics of transition-metal (TM) dihalides with either CdCl₂- or CdI₂-type structure.⁷

In the ESM the tensor components of $\epsilon_{\alpha\alpha}^{\infty}$ are directly related to the internal shell-core force constants g_{κ} ($\kappa = \pm 1$) and to the shell-shell Coulomb (YCY) and short-range repulsive (R) force-constant matrices.⁸ The local field, as obtained from lattice sums over all shell (Y_{κ}) and core charges, contains the important contributions of the static dipoles born by the halide ions, and reflects the appreciable anisotropy which is inherent in this class of layered compounds. This accounts for the deviations from the isotropic Clausius-Mossotti equation connecting $\epsilon(\infty)$ to the ion polarizabilities $\alpha_{\kappa} = Y_{\kappa}^2/g_{\kappa}$. The assessment of a standard set of ion polarizabilities having the property of transferability from one crystal to another of the same class—and possibly to ionic crystals of different classes—depends to a large extent on the exact microscopic rela-

tionship between α_{κ} and the experimental $\epsilon_{\text{xx}}^{\infty}$. The transferability of shell-model parameters, which is an important requirement for shell models, can be used to predict the phonon structure of solids when neutron data are not available.

In this work we want to compare the theoretical ESM values $\epsilon_{\text{xx}}^{\infty}$ to our experimental effective dielectric constants produced by optical transitions in the range 2–31 eV in Fe, Co, and Ni dichlorides and dibromides. To this aim, we present in Sec. II only some relevant optical data describing the kind of electronic transitions that contribute most importantly to the high-frequency dielectric constant together with some considerations about the unavoidable experimental approximation involved. A more complete study of the fundamental ultraviolet properties up to 31 eV will be reported in a planned, future paper.² In Sec. III we show that the previous ESM calculations based on the simplifying assumption of negligible polarizations for cations ($\alpha_{+} \sim 0$) and on Tessman-Kahn-Schockley (TKS) polarizabilities for anions⁹ yield values of $\epsilon_{\text{xx}}^{\infty}$ which are systematically smaller (10–20%) than the experimental values. Finally, we show that the discrepancy is practically removed if cation polarizabilities are taken into account and given the values derived by Shanker, Sharma, and Gupta (SSG) for 3d-metal oxides.¹⁰ This fact indicates, by the way, that TKS and SSG polarizabilities enjoy transferability. On the other hand, they fulfill the Clausius-Mossotti equation only roughly for dichlorides, whereas larger and larger deviations are observed for dibromides and di-iodides, as expected from the larger influence of static dipoles.

II. EXPERIMENTAL RESULTS

The optical response of Fe, Co, and Ni dihalides has been investigated throughout the near-ultraviolet region by means of synchrotron radiation from the 0.54-GeV storage ring Anneau de Collision d'Orsay (ACO). The stability and good vacuum ($\sim 10^{-10}$ mm Hg) conditions of the ACO storage ring have permitted the extension of near-normal incidence reflectance spectra up to 31 eV.¹⁻³ We used KK relations to generate the dielectric function $\hat{\epsilon}(E)$, which describes the optical properties. As an example, we show the real and imaginary parts of $\hat{\epsilon}(E) = \epsilon_1(E) + i\epsilon_2(E)$ for Fe, Co, and Ni dichlorides in Fig. 1. The dielectric constants for these crystals are small compared to those of typical semiconductors, such as silicon or germanium, indicating that the Coulomb interaction is correspondingly more effective. We see that the curves corresponding to absorption peaks in the lowest-energy region, below 10 eV, are oscillatorlike. These peaks correspond to charge-transfer excitons and transitions from the p -like valence band to the d -metal states, up to 6–7 eV, and to direct interband excitons around 8–9 eV. The onset of interband $p \rightarrow s$ transitions has been related to a weak absorption shoulder which occurs at the high-energy side of the first Γ exciton at 8.70–9 eV in TM chlorides.^{1,2} In the energy range 8–13 eV one essentially observes interband transitions from $3p$ levels of chlorine to empty s states of the conduction band. Plasma resonance effects occur around 18–19 eV, where $\epsilon_1(\hbar\omega_p) \simeq 0$ and a broad, strong maximum is observed in the spectra of the energy-loss functions $-\text{Im}\hat{\epsilon}^{-1}(E)$.²

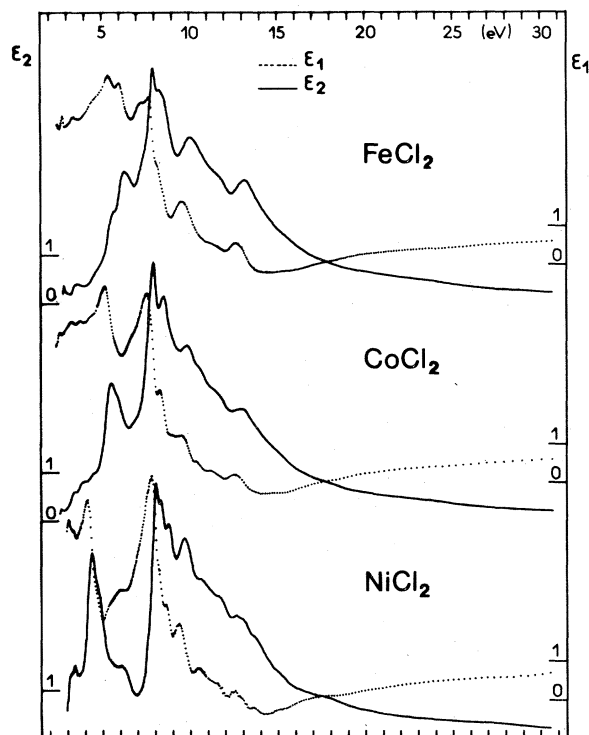


FIG. 1. Dielectric parameters ϵ_1 and ϵ_2 of NiCl_2 , CoCl_2 , and FeCl_2 at room temperature.

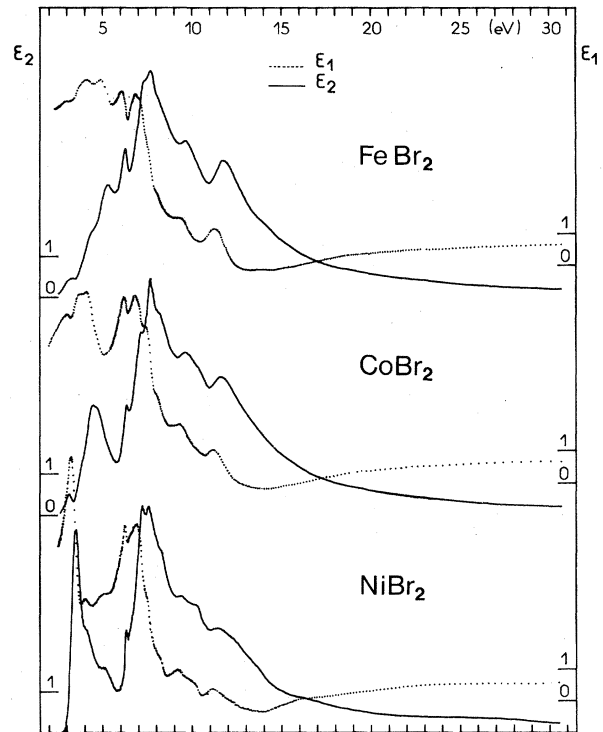


FIG. 2. Dielectric parameters ϵ_1 and ϵ_2 of NiBr_2 , CoBr_2 , and FeBr_2 at room temperature.

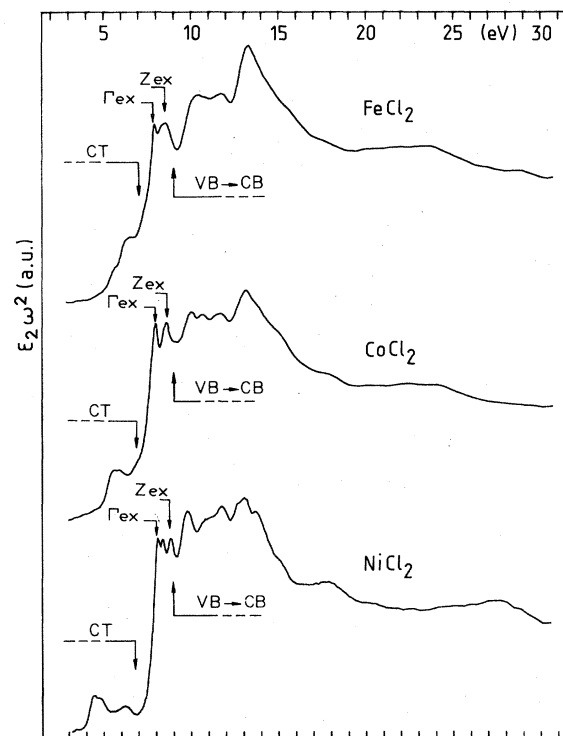


FIG. 3. Density-of-states function $\epsilon_2 E^2$ for NiCl_2 , CoCl_2 , and FeCl_2 derived from quasi-normal-incidence reflectance data at room temperature. The main assignments for NiCl_2 , valid also for Co and Fe chlorides, are taken from Refs. 1 and 2.

The following rapid decrease of the dielectric function $\epsilon_2(E)$ indicates that the oscillator strength associated with the valence electrons rapidly becomes exhausted in the (20–31)-eV region, but, as one penetrates the extreme ultraviolet region, new thresholds appear due to electron-core excitations.

The same considerations may be evolved for TM bromides, whose dielectric parameters are reported in Fig. 2 for sake of comparison. The previous assignments are then indicated in Figs. 3 and 4 where we present the optical excitation spectra of Fe, Co, and Ni dichlorides and dibromides, shown by the measured density of states. In particular, in dibromides, the optical transitions below the interband gap, which is around 8 eV, and above the gap, have the same characteristics as in chlorides, and these transitions may correspondingly be assigned on the grounds of the very similar band structure.^{1,2} We briefly are reminded that the valence and conduction bands are separated in TMH crystals by a forbidden gap which contains the 3*d* levels of the metal, quasilocalized and partially filled. Also, the valence and conduction bands are separated by a "forbidden gap" varying from ~8 eV in bromides to ~9 eV in chlorides, while the *p-d* gap is about 3–5 eV. Now, in order to discuss the dielectric and optical properties of semiconductors and metals, a number of useful relations are known which link the real and imaginary parts of the dielectric and optical functions. In particular, two sum rules involving $\epsilon_2(E)$ are valuable in analyzing the data throughout the ultraviolet region. It is usual, in these cases, to present the expressions for finite

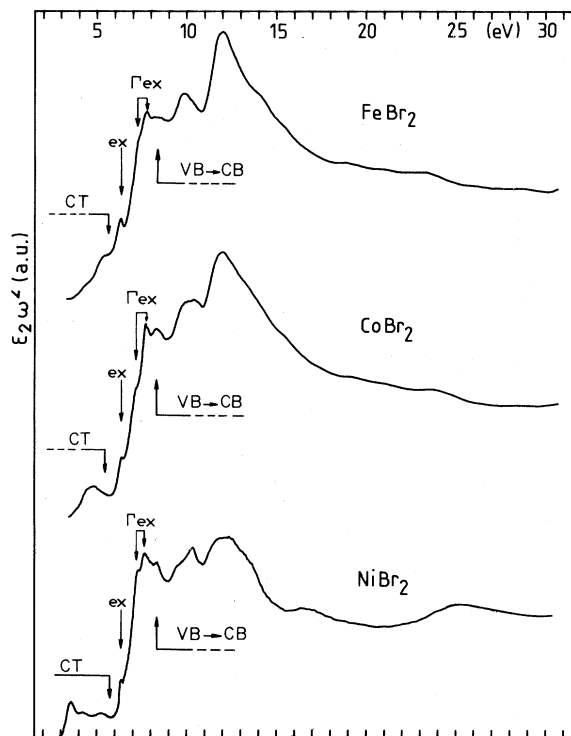


FIG. 4. Density-of-states function $\epsilon_2 E^2$ for NiBr_2 , CoBr_2 , and FeBr_2 derived from quasnormal-incidence reflectance data at room temperature. Assignments for bromides are also reported from Refs. 1 and 2.

intervals of integration and to use the random-phase-approximation (RPA) results for $\epsilon_2(E)$. Since we consider uniaxial crystals with the *c* optical axis along the *z* axis, it may be also useful to point out how to compare the dielectric tensor elements, obtained by ESM calculations, to the appropriate dielectric $\epsilon_{\alpha\alpha}^T(0, E)$ elements measured in the long-wavelength limit ($k \approx 0$), because the transverse (*T*) and longitudinal (*L*) dielectric functions are not equal for noncubic materials. In our case, the optical reflectance for light traveling (almost) parallel to the *z* axis determines $\epsilon_{xx}^T(0, E) = \epsilon_{yy}^T(0, E)$, which for long wavelengths should be equal to $\epsilon_{zz}^L(0, E)$ in the RPA, so that the appropriate tensor element to compare to experimental values is $\epsilon_{\text{eff}, xx}(E)$.

The first integral,

$$\epsilon_{\text{eff}}(E) = 1 + \frac{2}{\pi} \int_2^E \frac{\epsilon_2(E')}{E'} dE', \quad (1)$$

where *E* and *E'* are given in eV, defines the effective dielectric constant associated with optical transitions in the energy range 2–31 eV. This equation gives the static dielectric constant $\epsilon(0)$ below the reststrahlen frequency, if one takes into account the whole infrared lattice absorption in the integration. Otherwise, the optical dielectric constant $\epsilon(\infty)$ is obtained. In Figs. 5(a) and 6(a) we present plots of $\epsilon_{\text{eff}}(E)$ for chlorides and bromides, respectively. The strong variation of the steplike curves below 13–15 eV for chlorides and 12–13 eV for bromides results from the fact that $\epsilon_2(E)$ describes widespread al-

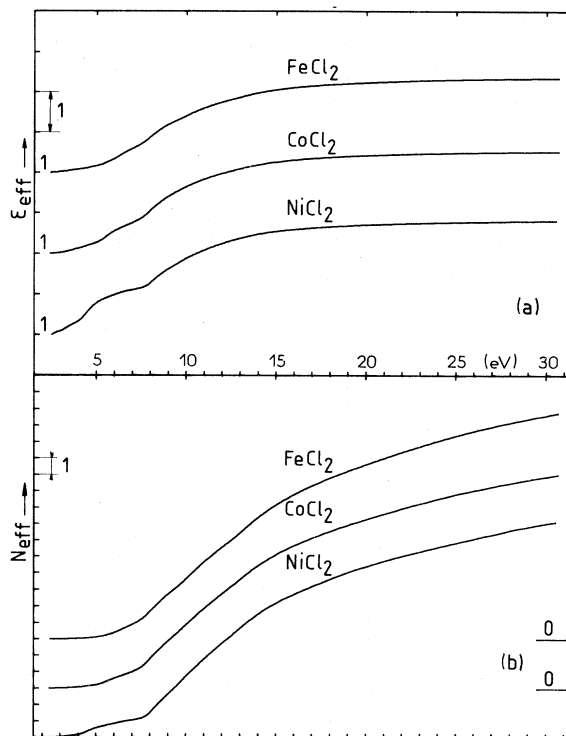


FIG. 5. (a) Effective dielectric constants and (b) the effective number of electrons per molecule vs *E* for Ni, Co, and Fe dichlorides are obtained from integration of experimental $\epsilon_2(E)$ using Eqs. (1) and (1'). The saturation value of $\epsilon_{\text{eff}}^{\infty} \approx \epsilon_{xx}^{\infty}$ reported in Table I is taken at 31 eV.

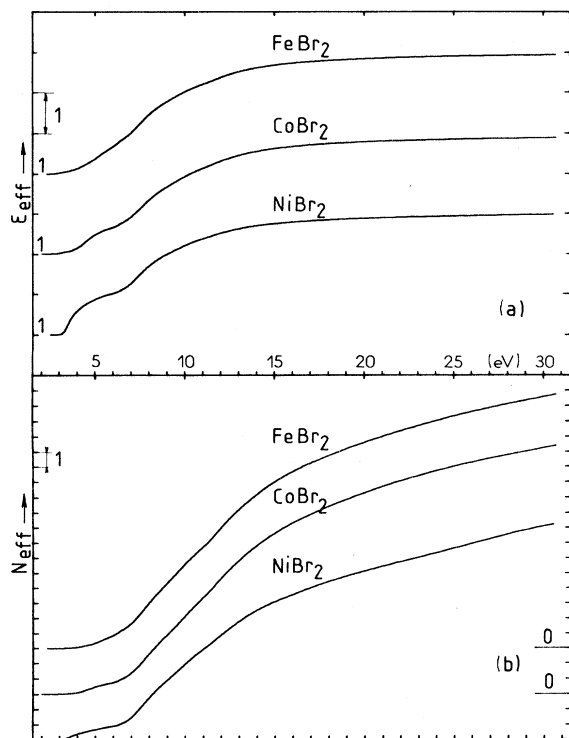


FIG. 6. (a) Effective dielectric constants and (b) the effective number of electrons per molecule vs E for Ni, Co, and Fe dibromides are obtained in the same way as in TM chlorides.

lowed transitions which give a rapid increase in $\epsilon_{\text{eff}}(E)$ as $\hbar\omega$ passes across the strong absorption p - d and p - s edges. Thus, it is possible to judge which transitions give the most prominent contribution to the high-frequency (electronic) dielectric constant for TMH crystals. From the tendency towards saturation at photon energies above 13–15 eV, it is clear that allowed charge-transfer ($p \rightarrow d$)

and interband ($p \rightarrow s$) transitions are mainly responsible for the value of ϵ_{eff} . On the contrary, the odd-phonon-assisted crystal-field ($d \rightarrow d$) transitions which occur below 2–3 eV do not contribute to ϵ_{eff} appreciably. Since we neglect in our analysis the contribution of the d - d transitions and the contributions of threshold which appear in the extreme ultraviolet region, we expect *a priori* that the “true” value of $\epsilon(\infty)$ should be higher than the measured one, i.e., $\epsilon_{\text{eff}}(E)$. How much higher the true value is can be inferred considering the case of K halides,⁶ where the saturation value of ϵ_{eff} —evaluated through KK relations in the energy range 5–25 eV—was compared to that of an independently measured dielectric constant above the reststrahlen frequency, with an excellent agreement (for example, see Fig. 5 of Ref. 6). This seems to rule out the importance of higher-energy contributions as well and make our approximation, involved in Eq. (1), a good one. The second integral evaluates $N_{\text{eff}}(E)$, the effective number of electrons which participate in the optical processes up to E ,

$$N_{\text{eff}}(E) = \frac{2m\epsilon_0}{\pi\hbar^2} v_c \int_2^E \epsilon_2(E') E' dE', \quad (1')$$

with E and E' in eV; v_c is the volume of the unit cell and the multiplicative factor is expressed in the International System of Units. The reported curves of $N_{\text{eff}}(E)$, in Figs. 5(b) and 6(b) when compared, for example, with the $\epsilon_2(E)$ spectra of Figs. 1 and 2, show that over 7–8 eV, more than two electrons contribute to the electronic transitions. This sudden increase of N_{eff} is in agreement with the onset of interband transitions. The region for $E \leq 7$ eV should then define the charge-transfer region. We note again a tendency towards saturation of the optical processes beyond 15–18 eV, in close correspondence with the behavior of the curves of $\epsilon_{\text{eff}}(E)$. The plots of $N_{\text{eff}}(E)$ should saturate at 18–20, as there are 6–8 electrons in the metal $3d$ levels and six electrons for the halogen ions. We finally make some considerations on the accuracy of this

TABLE I. Polarizabilities and ESM-calculated dielectric constants compared to experimental ϵ_{eff} and to values derived from isotropic CM equation.

| | α_-^a (\AA^3) | α_+^b | ϵ_{zz}^∞ (ESM) | ϵ_{xx}^∞ | $\epsilon_{\text{eff},xx}$ (Expt.) | ϵ^∞ [Eq. (5)] |
|-------------------|------------------------------------|--------------|---------------------------------|------------------------|---------------------------------------|--------------------------------|
| FeCl ₂ | 2.974 | 0 | 2.623 | 2.710 | | |
| | | 1.13 | 3.26 | 3.34 | 3.35 | 3.528 |
| CoCl ₂ | 2.974 | 0 | 2.697 | 2.784 | | |
| | | 0.99 | 3.22 | 3.31 | 3.50 | 3.573 |
| NiCl ₂ | 2.974 | 0 | 2.812 | 2.919 | | |
| | | 0.89 | 3.32 | 3.43 | 3.75 | 3.762 |
| FeBr ₂ | 4.130 | 0 | 3.194 | 3.344 | | |
| | | 1.13 | 3.68 | 3.83 | 3.94 | 4.405 |
| CoBr ₂ | 4.130 | 0 | 3.342 | 3.524 | | |
| | | 0.99 | 3.73 | 3.91 | 3.89 | 4.663 |
| NiBr ₂ | 4.130 | 0 | 3.635 | 3.638 | | |
| | | 0.89 | 3.91 | 3.92 | 3.98 | 4.492 |
| VI ₂ | 6.199 | 0 | 3.480 | 3.703 | | |
| | | 1.85 | 3.99 | 4.22 | c | 6.152 |

^aTKS values (Ref. 9).

^bSSG values (Ref. 10).

^c $\epsilon_{\text{eff},xx} = 4.4$ for NiI₂, 4.0 for CoI₂, and 3.8 for FeI₂ (from Ref. 13).

type of analysis which depends sensitively on the absolute values of $\epsilon_2(E)$, and hence of the reflectance curves, which have not been reported here. In our case, we have estimated that the accuracy in the absolute value of the reflectivity and its reproducibility in the course of several runs on freshly cleaved single crystals was below 5%.

III. ESM RESULTS

The ESM expression for the high-frequency dielectric tensor is⁸

$$\epsilon_{\alpha\alpha}^{\infty} = 1 + 4\pi v_c^{-1} \sum_{\kappa, \kappa'} Y_{\kappa}(S^{-1})_{\kappa\alpha, \kappa'\alpha} Y_{\kappa'}, \quad (2)$$

where v_c is the volume of the unit cell, and

$$S^{-1} = g^{-1} [1 + (YCY + R)g^{-1}]^{-1} \quad (3)$$

represents the effective electronic polarizability. The structure of $YS^{-1}Y$ consists of the product of single-ion polarizabilities

$$\alpha_{\kappa} = Y_{\kappa}^2 / g_{\kappa}, \quad (4)$$

times the local-field correction—the resonant denominator in square brackets in Eq. (3)—which contains the Coulomb and repulsive interactions with the surrounding ions. It is this factor which bears the information on the static dipoles and the structural anisotropy.¹¹

The calculated values of ϵ_{zz}^{∞} and ϵ_{xx}^{∞} are listed in Table I for TKS values of α_{-} and either $\alpha_{+} = 0$ or α_{+} equal to SSG values. The second set of calculated ϵ_{xx}^{∞} values is in very good agreement with the experimental $\epsilon_{\text{eff}, xx}$, whereas the values for $\alpha_{+} = 0$ are 10–20% too small. In this regard, neglecting the cation polarizability is a poor approximation, as argued by Kuindersma in his discussion on the TM di-iodides.¹² With regard to VI_2 , we do not have experimental data, but the calculated value $\epsilon_{xx} = 4.22$ scales well with the experimental values for NiI_2 , CoI_2 , and FeI_2 , whose saturation values are 3.8, 4, and 4.4, respectively.¹³

Since the anisotropy of $\epsilon(\infty)$ turns out to be relatively small, one may argue that the isotropic Clausius-Mossotti (CM) equation,

$$\frac{\epsilon^{\infty} - 1}{\epsilon^{\infty} + 2} = \frac{4\pi}{3v_c} (2\alpha_{-} + \alpha_{+}), \quad (5)$$

would be approximately fulfilled by the sets of TKS and SSG polarizabilities. Actually the values of $\epsilon(\infty)$ obtained from (5) (Table I, column 7) are only slightly larger

than the experimental $\epsilon_{\text{eff}, xx}$ for chlorides, but stronger deviations occur for dibromides and VI_2 . This means that the apparent anion polarizability as deduced from the CM equation does not increase from Cl^{-} through I^{-} as much as for TKS values. Such a greater apparent rigidity of larger ions can be ascribed to the existence of static dipoles. Parenthetically, we note that the CM values of $\epsilon(\infty)$ for di-iodides are in the range of values experimentally obtained for CoI_2 and NiI_2 from KK analysis and oscillator fits applied to infrared data by Kuindersma,¹² but altogether the latter values are fairly larger than the values obtained from synchrotron-radiation reflection spectroscopy. At present we are inclined to think that one possible origin of such systematic discrepancy between the results obtained by the two above experimental methods is due to the omission of non-negligible contributions in the evaluation of $\epsilon(\infty)$. For instance, if one disregards some coupled photon-phonon modes, which in ionic crystals increase the dielectric function $\epsilon(E)$ —whereby $\epsilon(\infty)$ is derived by the difference between the static dielectric constant $\epsilon(0)$ and the first-order (plus higher-order) coupled modes—one may get an overestimated value for the high-frequency constant $\epsilon(\infty)$. This would happen if multi-phonon processes, among which two-phonon processes are prominent, are not taken care of in the experiments. For example, in layered vanadium dihalides absorption peaks due to two-phonon processes are observed on the high-energy side of the main infrared absorption peak (see Fig. 5 of Ref. 14). The main mechanism responsible for the two-phonon infrared absorption in polar crystals consists in the direct coupling of the photon of a two-phonon state via the second-order dipole moment.¹⁵ This mechanism is, in general, negligible in isotropic ionic crystals (alkali halides), but it can be important in anisotropic TMH crystals as a consequence of the small dispersion of the phonon-optical branches.⁷

ACKNOWLEDGMENTS

The authors (J.T. and I.P.) thank the technical staff of the Laboratoire d'Utilisation du Rayonnement Electromagnétique for their assistance during experiments, and one of us (I.P.) also gratefully acknowledges the Centre National de la Recherche Scientifique for financial support during his stay at the Université de Paris-Sud. In particular, another of us (G.B.) thanks Dr. R. Zeyer (Max-Planck Institut für Festkörperforschung, Stuttgart, Federal Republic of Germany) for useful discussions.

¹I. Pollini, J. Thomas, G. Jezequel, J. C. Lemonnier, and R. Mamy, *Phys. Rev. B* **27**, 1303 (1983).

²J. Thomas, G. Jezequel, J. C. Lemonnier, and I. Pollini (unpublished); see also I. Pollini *et al.*, in *Europhysics Conference Abstracts*, edited by V. Heine (Cambridge University Press, London, 1983), Vol. 6, p. 425.

³J. Thomas, G. Jezequel, and J. C. Lemonnier, in *Proceedings of the VIth International Conference on Vacuum Ultraviolet Radiation Physics, Virginia, 1980*, Extended Abstracts No. I-46 (unpublished), p. 46.

⁴P. Nozières and D. Pines, *Phys. Rev.* **113**, 1254 (1959).

⁵H. R. Philipp and H. Ehrenreich, *Phys. Rev.* **129**, 1550 (1963).

⁶H. R. Philipp and H. Ehrenreich, *Phys. Rev.* **131**, 2016 (1963).

⁷G. Benedek and A. Frey, *Phys. Rev. B* **21**, 2482 (1980).

⁸A. Frey and R. Zeyher, *Solid State Commun.* **28**, 435 (1978).

⁹J. R. Tessman, A. H. Kahn, and W. Shockley, *Phys. Rev.* **92**, 890 (1953).

¹⁰J. Shanker, H. P. Sharma, and B. R. K. Gupta, *Solid State Commun.* **21**, 903 (1977).

¹¹A. Frey, Ph.D. thesis, University of Stuttgart, 1977.

- ¹²S. R. Kuindersma, *Phys. Status Solidi B* 107, K163 (1981);
Ph.D. thesis, University of Gröningen, 1980.
- ¹³I. Pollini, J. Thomas, A. Lenselink, and J. C. Lemonnier, *Annals of the Israel Physical Society* (Hilger, Bristol, 1983), Vol. 6, p. 255.
- ¹⁴W. Bauhofer, G. Güntherhodt, E. Anastassakis, A. Frey, and G. Benedek, *Phys. Rev.* 22, 5873 (1980).
- ¹⁵J. M. Ziman, *Principles of the Theory of Solids* (Cambridge University Press, London, 1964), p. 233.